Multi-channel quantum parameter estimation

Liying BAO[1,2], Bo QI[1,2*], Yabo WANG[1,2], Daoyi DONG[3] & Rebing WU[4]

[1]*Key Laboratory of Systems and Control, Academy of Mathematics and Systems Science,
Chinese Academy of Sciences, Beijing 100190, China;*
[2]*University of Chinese Academy of Sciences, Beijing 100049, China;*
[3]*School of Engineering and Information Technology, University of New South Wales,
Canberra ACT 2600, Australia;*
[4]*Department of Automation, Tsinghua University, Beijing 100084, China*

Abstract   The aim of quantum metrology is to exploit quantum effects to improve the precision of parameter estimation beyond its classical limit. In this paper, we investigate the quantum parameter estimation problem with multiple channels. It is related but not limited to the following two important and practical quantum metrology problems: (i) Quantum enhanced metrology with control, whose aim is to improve the precision of quantum sensing by utilizing feedback or open-loop control; (ii) Practical quantum metrology where the underlying evolution of quantum probes may change from a unitary dynamics to an open system dynamics, owing to the inevitable decoherence during the quantum sensing operation. For various kinds of quantum multiple channels, the corresponding quantum channel Fisher information is derived. To demonstrate the results, some illustrative examples are given.

Keywords   quantum metrology, quantum parameter estimation, multi-channel, quantum Fisher information

1   Introduction

High precision measurement of unknown parameters has been one of the pivotal tasks in science and technology [1–43]. A typical measurement procedure consists of a generic sequence of probe initialization, and the parameter encoding through a channel that is usually realized by a parameter-dependent dynamical evolution, following which the output is measured for an appropriate estimation of the interested unknown parameter [4]. To achieve the highest admissible precision, one needs to make the best use of available resources and design optimal schemes to reach the limit [22–43].

Denote by x the unknown parameter to be measured, if a specific measurement is fixed, the ultimate precision of any unbiased estimator is bounded below by the Fisher information $I(x)$ in the form of the well-known Cramér-Rao inequality [4–8, 29–31, 44, 45]. The Fisher information $I(x)$ quantifies the maximum amount of information about the true value of x that can be extracted from the selected measurement procedure, which is jointly determined by the initial state of the probe, the parameter encoding channel, and the measurement scheme.

More fundamentally, the precision of parameter estimation is determined by the physical mechanism behind the estimation process. It was shown that by exploiting quantum effects, the precision limit of parameter estimation can go beyond its classical counterpart, leading to the emerging technology of quantum metrology [23–35]. From the view of quantum mechanics, any classical measurement scheme can be considered as a projective measurement, and thus one can obtain the quantum Fisher information $J(x)$ by maximizing the Fisher information $I(x)$ over all possible measurement strategies allowed by quantum mechanics [4, 43–46]. This figure of merit $J(x)$, which depends upon the state of the probe before the measurement, thus characterizes the maximum amount of information that can be extracted about the

---

* Corresponding author (email: qibo@amss.ac.cn)

unknown parameter x using the best quantum measurement strategies. The corresponding Cramér-Rao inequality in terms of $J(x)$ sets the best precision limit that may be attained for any unbiased estimator under a given initial state of the probe and a fixed parameter encoding channel.

The precision of quantum parameter estimation can be further improved by maximizing the quantum Fisher information $J(x)$ over all initial states of the probe [4, 6, 47]. Typically, by utilizing quantum recourses such as entanglement and squeezing, the lower bound can be significantly reduced compared with classical strategies [25–27, 47]. For instance, in classical metrology, the estimation error generally scales as $O(1/\sqrt{N})$, where N is the number of probes used in the measurements. By exploiting quantum resources, the error scaling can be greatly reduced to $O(1/N)$ [4–6, 27–31, 48].

Under the optimal quantum measurement and a given initial state of the probe, the quantum Fisher information $J(x)$ is only related to the parameter encoding channel. In this regard, we also call $J(x)$ as the quantum channel Fisher information. The calculation of the quantum Fisher information of a given channel has been widely investigated in [4–8, 29–31]. Physically, the encoding channel can be manipulated by external controls, and thus one can optimize the controls to improve $J(x)$. One can even apply feedback control to alter the total dynamics to improve the precision limit. For example, in [30], an optimal feedback scheme was utilized to obtain a universal time scaling for the precision limit. In [26], it was demonstrated that a sequential feedback scheme can outperform the parallel scheme for Hamiltonian parameter estimation. To obtain the enhanced precision with feedback, a key assumption was made that the involved controls take negligible time, which is a valid assumption in some physical settings. However, for general setups, this assumption is usually invalid and the encoding dynamics must be taken into account in the duration of controls.

In practice, the control (e.g., via arbitrary waveform generator in microwave regime) is often generated in the form of bounded piecewise-constant pulses, the entire quantum dynamics can be viewed as sending the probe through a sequence of encoding channels that are determined by these constant sub-pulses. Thus a natural and important question arises: how to calculate the quantum Fisher information of a sequence of multiple quantum channels. From a practical viewpoint, it is also important to investigate the multi-channel quantum metrology. In presence of inevitable noises, quantum system dynamics cannot be modeled as a strictly unitary process. As a matter of fact, a quantum system must be treated as an open system once the time duration is comparable with the coherence time. However, as a valuable resource in quantum metrology, the sensing time is expected to be as long as possible for better precision. In the case where the sensing time is longer than the coherence time, the measurement process can be formulated as a multi-channel quantum metrology problem, i.e., a unitary channel whose duration is much smaller than the coherence time, which is followed by a non-unitary encoding channel. The quantum channel Fisher information of the total encoding channel and the first unitary part only can be calculated to compare the corresponding precision limits.

In this paper, we address and calculate the quantum Fisher information with various kinds of multiple channels. The paper is organized as follows. In Section 2, we introduce the tools to be utilized to calculate the quantum channel Fisher information and set up the problem under consideration. Then in Section 3, we first consider the simplest case, i.e., the multiple channels are two sequential unitary channels, and then generalize the result to an arbitrary number of sequential unitary channels. Section 4 investigates the case where a unitary channel is followed by a non-unitary channel. Section 5 concludes the paper.

2 Quantum Fisher information and problem statement

A general measurement procedure of an unknown parameter is shown in Figure 1. The probe is first prepared in a known initial state ρ_0, and then evolves for a duration t, whose dynamics depend on the unknown parameter x in a parametric way. This process can be viewed as the probe being sent through a parameter encoding channel ε_x. A set of quantum measurements $\{E_y\}$, represented by positive operator valued measures, is performed on the final state of the channel. The occurrence probability of the result y is $p(y|x) = \text{Tr}(E_y\rho_x)$. Based on the distribution of the obtained measurement results, an estimate $\hat{x}$ of the unknown parameter x can be given through a proper algorithm such as the maximum likelihood method [49] or the linear regression estimation [50, 51].

For any unbiased estimator, the precision limit is bounded below by the Fisher information $I(x)$ in the
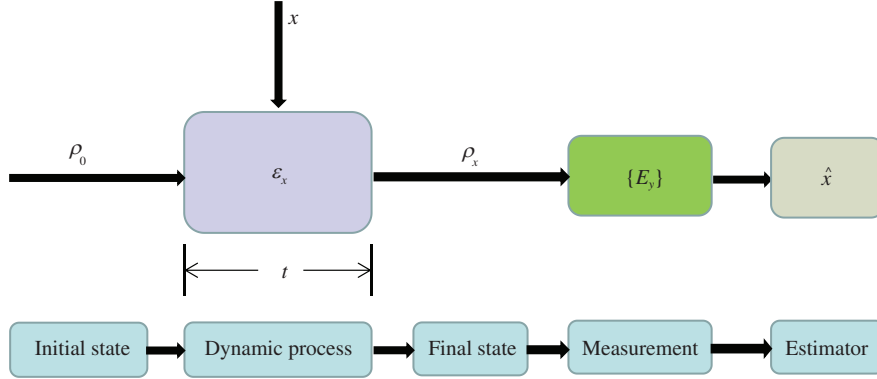
Figure 1 (Color online) Schematic for quantum parameter estimation. The probe prepared in an initial state ρ_0 is sent through a quantum encoding channel ε_x for a time duration t. After that, a measurement is implemented on the final state, and an estimate $\hat{x}$ of the parameter x is given based on the measurement results.

form of the Cramér-Rao inequality

$$\delta\hat{x} \equiv \sqrt{\langle(\hat{x} - x)^2\rangle} \geqslant \frac{1}{\sqrt{I(x)}},$$

where

$$I(x) = \sum_y p(y|x) \left(\frac{\partial \ln p(y|x)}{\partial x}\right)^2.$$

As explained in Section 1, we can first maximize the Fisher information $I(x)$ over all possible measurement strategies allowed by quantum mechanics to obtain the quantum Fisher information of the state ρ_x as $J(\rho_x) = J(\varepsilon_x(\rho_0))$ [46]. The corresponding Cramér-Rao inequality gives

$$\delta\hat{x} \geqslant \frac{1}{\sqrt{J(\rho_x)}}.$$

Since the quantum state Fisher information $J(\rho_x)$ depends on the initial state ρ_0 of the probe, the precision limit can be further improved by maximizing $J(\rho_x)$ over all initial states of the probe [47, 52]. For a unitary channel, i.e., $\varepsilon_x = U_x$, the quantum channel Fisher information of U_x is given as [30]

$$J(U_x) = \lim_{dx \to 0} \frac{4C_\theta^2(U_x^\dagger U_{x+dx})}{dx^2}, \tag{1}$$

where $C_\theta(U)$ is the maximal angle that the unitary operater U can rotate a state away from itself. The operator $\dagger$ denotes the conjugate transpose. It can be derived that $\cos[C_\theta(U)] = \min_\rho F(\rho, U\rho U^\dagger)$, where the fidelity $F(\rho_1, \rho_2) = \text{Tr}\sqrt{\rho_1^{\frac{1}{2}}\rho_2\rho_1^{\frac{1}{2}}}$. The detailed definition of $C_\theta(U)$ for any unitary operator U can be found in [52]. For an $m \times m$ unitary matrix U, denote $e^{-i\theta_j}$ as the eigenvalues of U, where $\theta_j \in (-\pi, \pi]$ for $j = 1, \ldots, m$. If

$$\theta_{\min} = \theta_1 \leqslant \theta_2 \leqslant \cdots \leqslant \theta_m = \theta_{\max}$$
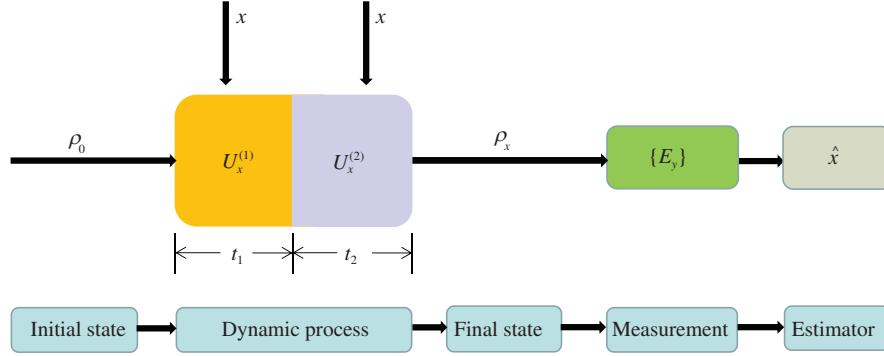
are arranged in ascending order, then we have [52]

$$C_\theta(U) = \frac{\theta_{\max} - \theta_{\min}}{2}, \quad \text{when} \quad \theta_{\max} - \theta_{\min} \leqslant \pi. \tag{2}$$

This result combined with (1) will be employed to derive our main results in Section 3.

For a non-unitary channel, i.e., $\varepsilon_x(\rho) = \sum_i k_i(x)\rho k_i^\dagger(x)$, where the Kraus operators $\{k_i(x)\}$ satisfy $\sum_i k_i^\dagger(x)k_i(x) = I$, the quantum channel Fisher information of ε_x is given by [47]

$$J(\varepsilon_x) = \lim_{dx \to 0} \frac{8(1 - \max_{||W|| \leqslant 1} \frac{1}{2}\lambda_{\min}(K_W + K_W^\dagger))}{dx^2}, \tag{3}$$

Figure 2 (Color online) Schematic for quantum parameter estimation under two unitary channels. The probe prepared in a known initial state ρ_0, first evolves as $U_x^{(1)} = \mathrm{e}^{-\frac{i}{\hbar} H_x^{(1)} \cdot t_1}$ driven by the Hamiltonian $H_x^{(1)}$ for a duration t_1 and then evolves as $U_x^{(2)} = \mathrm{e}^{-\frac{i}{\hbar} H_x^{(2)} \cdot t_2}$ with the underlying Hamiltonian $H_x^{(2)}$ for a duration t_2. After that, a measurement is implemented on the final state, and based on the measurement results an estimate $\hat{x}$ of the parameter x is given.

where $\lambda_{\min}(A)$ denotes the minimal eigenvalue of matrix A, $K_W = \sum_{i,j} w_{ij} k_i^\dagger(x) k_j(x + dx)$, and w_{ij} is the ij-th element of the matrix W which satisfies $\|W\| \leqslant 1$ (the matrix norm $\|\cdot\|$ is referred to as the maximum singular value). This formula will be applied to obtain our main results in Section 4.

Let us see how the encoding channel affects the precision limit. Usually, the unknown parameter x is imprinted on the probe through a fixed Hamiltonian H_x during the encoding process, even though in the cases where feedback controls are involved. This is owing to the key assumption made therein that feedback controls take negligible time. However, for general physical settings, this assumption is not valid, leading to the fact that for different control periods, the control-induced-evolution together with the encoding dynamics are different. As explained in Section 1, the total feedback-involved-encoding process can be dealt with from a new viewpoint. Firstly, it is well known that any continuous control can be arbitrarily approximated by piecewise controls corresponding to a sequence of quantum encoding channels. Secondly, the realistic open system dynamics may introduce additional non-unitary channels. In the following, we will derive the quantum channel Fisher information of multi-unitary-channels, and the case where the multiple channels consist of a unitary channel followed by a non-unitary channel.

3 Quantum channel Fisher information of multi-unitary-channel

3.1 The case with two unitary channels

In this subsection, we focus on the simplest case where the multiple channels are two unitary channels. To be specific, as shown in Figure 2, the probe prepared in state ρ_0 is first sent through the encoding channel $U_x^{(1)} = \mathrm{e}^{-\frac{i}{\hbar} H_x^{(1)} \cdot t_1}$, and then the channel $U_x^{(2)} = \mathrm{e}^{-\frac{i}{\hbar} H_x^{(2)} \cdot t_2}$. By the end of the entire dynamics, the probe state becomes $\rho_x = U_x \rho_0 U_x^\dagger$, where $U_x = U_x^{(2)} U_x^{(1)}$ is the total encoding channel. Note that for $i = 1, 2$, the Hamiltonian $H_x^{(i)}$ can be decomposed as $H_x^{(i)} = H_x^{(0)} + H_c^{(i)}$, where $H_x^{(0)}$ is the encoding Hamiltonian, and $H_c^{(i)}$ is the i-th control Hamiltonian, the time t_i is actually the duration of the control Hamiltonian $H_c^{(i)}$.

Before deriving the quantum channel Fisher information, we give some notations. Firstly, denote $J(U_x^{(i)})$ and $J(U_x)$ as the quantum channel Fisher information for the unitary channel $U_x^{(i)}$ and the entire channel U_x, respectively. Secondly, define

$$h_x^{(1)} \triangleq i(\partial_x U_x^{(1)}) U_x^{(1)\dagger}, \quad h_x^{(2)} \triangleq i U_x^{(2)\dagger} \partial_x U_x^{(2)}. \tag{4}$$

Thirdly, let $\lambda_{\max}(A)$ and $\lambda_{\min}(A)$ denote the maximal and minimal eigenvalues of a matrix A, respectively. The quantum channel Fisher information can be calculated as Theorem 1.

Theorem 1. The quantum Fisher information of the total encoding channel U_x and the channel $U_x^{(1)}$ are $J(U_x) = [\lambda_{\max}(h_x^{(1)} + h_x^{(2)}) - \lambda_{\min}(h_x^{(1)} + h_x^{(2)})]^2$ and $J(U_x^{(1)}) = [\lambda_{\max}(h_x^{(1)}) - \lambda_{\min}(h_x^{(1)})]^2$, respectively. Moreover, if

$$[\lambda_{\max}(h_x^{(1)} + h_x^{(2)}) - \lambda_{\min}(h_x^{(1)} + h_x^{(2)})] \geqslant [\lambda_{\max}(h_x^{(1)}) - \lambda_{\min}(h_x^{(1)})],$$

then $J(U_x) \geqslant J(U_x^{(1)})$.

Proof. To obtain the quantum Fisher information of the entire channel U_x, according to (1), one needs to calculate $C_\theta(U_x^{(1)\dagger} U_x^{(2)\dagger} U_{x+dx}^{(2)} U_{x+dx}^{(1)})$, where dx is an infinitesimal change of x.

Note that the set of eigenvalues of $U_x^{(1)\dagger} U_x^{(2)\dagger} U_{x+dx}^{(2)} U_{x+dx}^{(1)}$ is the same as that of $U_x^{(2)\dagger} U_{x+dx}^{(2)} U_{x+dx}^{(1)} U_x^{(1)\dagger}$. Combining (1) and (2), the quantum Fisher information $J(U_x)$ of the total encoding channel U_x can be described as

$$
\begin{aligned}
J(U_x) &= \lim_{dx \to 0} \frac{4C_\theta^2(U_x^{(1)\dagger} U_x^{(2)\dagger} U_{x+dx}^{(2)} U_{x+dx}^{(1)})}{dx^2} \\
&= \lim_{dx \to 0} \frac{4C_\theta^2(U_x^{(2)\dagger} U_{x+dx}^{(2)} U_{x+dx}^{(1)} U_x^{(1)\dagger})}{dx^2}.
\end{aligned}
\tag{5}
$$

Since $U_{x+dx}^{(1)} = U_x^{(1)} + \partial_x U_x^{(1)} dx + o(dx)$, we have

$$
\begin{aligned}
U_{x+dx}^{(1)} U_x^{(1)\dagger} &= I + (\partial_x U_x^{(1)}) U_x^{(1)\dagger} dx + o(dx) \\
&= I - i(i\partial_x U_x^{(1)}) U_x^{(1)\dagger} dx + o(dx) \\
&= \exp(-i h_x^{(1)} dx) + o(dx).
\end{aligned}
\tag{6}
$$

To calculate $h_x^{(1)}$, we apply the following integral formula for the derivative of an operator exponential [48,53]

$$
\frac{\partial}{\partial x} \exp\left(-\frac{i}{\hbar} H_x \cdot t\right) = -i \int_0^t \exp\left(-\frac{i}{\hbar} H_x \cdot s\right) \left(\frac{\partial H_x}{\partial x}\right) \exp\left(\frac{i}{\hbar}(s-t) H_x\right) ds,
$$

which gives the expression of $h_x^{(1)}$ as

$$
h_x^{(1)} = \int_0^{t_1} \exp\left(-\frac{i}{\hbar} s H_x^{(1)}\right) \left(\frac{\partial H_x^{(1)}}{\partial x}\right) \exp\left(\frac{i}{\hbar} s H_x^{(1)}\right) ds.
\tag{7}
$$

In the same way, $U_x^{(2)\dagger} U_{x+dx}^{(2)}$ can be expressed as

$$
\begin{aligned}
U_x^{(2)\dagger} U_{x+dx}^{(2)} &= I + U_x^{(2)\dagger}(\partial_x U_x^{(2)}) dx + o(dx) \\
&= I - i(i U_x^{(2)\dagger}(\partial_x U_x^{(2)})) dx + o(dx) \\
&= \exp(-i h_x^{(2)} dx) + o(dx),
\end{aligned}
$$

where $h_x^{(2)} = i U_x^{(2)\dagger} \partial_x U_x^{(2)}$ can be expressed in the integral form

$$
h_x^{(2)} = \int_0^{t_2} \exp\left(\frac{i}{\hbar} s H_x^{(2)}\right) \left(\frac{\partial H_x^{(2)}}{\partial x}\right) \exp\left(-\frac{i}{\hbar} s H_x^{(2)}\right) ds.
$$

Since $e^{A+B} = e^A e^B e^{-\frac{1}{2}[A,B]} \cdots$ [54], we have

$$
\begin{aligned}
U_x^{(2)\dagger} U_{x+dx}^{(2)} U_{x+dx}^{(1)} U_x^{(1)\dagger} &= e^{-i h_x^{(2)} dx} e^{-i h_x^{(1)} dx} + o(dx) \\
&= e^{-i(h_x^{(1)} + h_x^{(2)}) dx} + o(dx),
\end{aligned}
$$

in which the higher-order terms are neglected. By (2), we have

$$
\begin{aligned}
C_\theta(U_x^{(1)\dagger} U_x^{(2)\dagger} U_{x+dx}^{(2)} U_{x+dx}^{(1)}) &= C_\theta(U_x^{(2)\dagger} U_{x+dx}^{(2)} U_{x+dx}^{(1)} U_x^{(1)\dagger}) \\
&= \frac{\lambda_{\max}(h_x^{(1)} + h_x^{(2)}) dx - \lambda_{\min}(h_x^{(1)} + h_x^{(2)}) dx + o(dx)}{2}.
\end{aligned}
\tag{8}
$$

Thus combining (5) and (8), we obtain the quantum Fisher information of the entire encoding channel as follows:

$$
J(U_x) = [\lambda_{\max}(h_x^{(1)} + h_x^{(2)}) - \lambda_{\min}(h_x^{(1)} + h_x^{(2)})]^2.
\tag{9}
$$

Let us turn to the quantum information of the channel $U_x^{(1)}$, i.e., only the first unitary part of the total channel is used. By (1), (2) and (6), it is clear that

$$
\begin{aligned}
J(U_x^{(1)}) &= \lim_{dx \to 0} \frac{4C_\theta^2(U_x^{(1)\dagger} U_{x+dx}^{(1)})}{dx^2} \\
&= \lim_{dx \to 0} \frac{4C_\theta^2(U_{x+dx}^{(1)} U_x^{(1)\dagger})}{dx^2} \\
&= [\lambda_{\max}(h_x^{(1)}) - \lambda_{\min}(h_x^{(1)})]^2.
\end{aligned} \tag{10}
$$

This is actually a well-known result [1,30,47]. Thus, by (9) and (10), once the following inequality holds:

$$
[\lambda_{\max}(h_x^{(1)} + h_x^{(2)}) - \lambda_{\min}(h_x^{(1)} + h_x^{(2)})] \geqslant [\lambda_{\max}(h_x^{(1)}) - \lambda_{\min}(h_x^{(1)})], \tag{11}
$$

we have

$$
J(U_x) \geqslant J(U_x^{(1)}).
$$

Remark 1. Note that the dependence of $h_x^{(1)}$ in (7) on the Hamiltonian $H_x^{(1)}$ is highly nonlinear. However, when $H_x^{(1)}$ commutes with $\frac{\partial}{\partial x} H_x^{(1)}$, we have $h_x^{(1)} = t_1 \cdot \partial_x H_x^{(1)}$ according to (7). This can be satisfied under the following two conditions:

- $H_x^{(1)} = \sum_n P_n(x) H^n$, where $P_n(x)$ is a function of x, H is a fixed Hamiltonian, and n is an arbitrary positive integer;

- $H_x^{(1)} = Q^{-1} \begin{pmatrix} \lambda_1(x) & & \\ & \ddots & \\ & & \lambda_n(x) \end{pmatrix} Q,$

where $\lambda_i(x)$ depends on the parameter x, while Q is an invertible matrix independent of x.

Remark 2. It is worth pointing out that the inequality (11) does not always hold even in the case where $H_x^{(1)} = H_x^{(2)}$. As an illustration, let $H_x^{(1)} = H_x^{(2)} = B[\sin(x)\sigma_1 + \cos(x)\sigma_3]$, where $\sigma_1 = \begin{pmatrix} 0 & 1 \\ 1 & 0 \end{pmatrix}$ and $\sigma_3 = \begin{pmatrix} 1 & 0 \\ 0 & -1 \end{pmatrix}$ are the Pauli matrices. It can be calculated that the quantum Fisher information of the channel U_x is $J(U_x) = 4\sin^2(Bt)$, which oscillates with the sensing time. Thus simply extending the sensing time may not improve the quantum Fisher information.

Now we give a sufficient condition for the inequality (11) to be held. Suppose that the dimension of the quantum probe system is n. Since the matrices $h_x^{(1)}$ and $h_x^{(2)}$ are Hermitian, their eigenvalues are real. Denote $\lambda_j(h_x^{(i)})$, $1 \leqslant j \leqslant n$, as the eigenvalues of matrix $h_x^{(i)}$ for $i = 1, 2$, and arrange them in ascending order such that $\lambda_1(h_x^{(i)}) \leqslant \lambda_2(h_x^{(i)}) \leqslant \cdots \leqslant \lambda_n(h_x^{(i)})$. Similarly, the eigenvalues of $h_x^{(1)} + h_x^{(2)}$ can be expressed as $\lambda_1(h_x^{(1)} + h_x^{(2)}) \leqslant \lambda_2(h_x^{(1)} + h_x^{(2)}) \leqslant \cdots \leqslant \lambda_n(h_x^{(1)} + h_x^{(2)})$. We have Proposition 1.

Proposition 1. If $[\lambda_n(h_x^{(2)}) - \lambda_1(h_x^{(2)})] \geqslant 2[\lambda_n(h_x^{(1)}) - \lambda_1(h_x^{(1)})]$, then $J(U_x) \geqslant J(U_x^{(1)})$.

Proof. The eigenvalues of $h_x^{(1)} + h_x^{(2)}$ have the following relationships with $h_x^{(1)}$ and $h_x^{(2)}$ as [55],

$$
\lambda_n(h_x^{(1)} + h_x^{(2)}) \geqslant \lambda_1(h_x^{(1)}) + \lambda_n(h_x^{(2)}), \tag{12}
$$

and

$$
\lambda_1(h_x^{(1)} + h_x^{(2)}) \leqslant \lambda_n(h_x^{(1)}) + \lambda_1(h_x^{(2)}). \tag{13}
$$

According to (12) and (13), we have

$$
\lambda_n(h_x^{(1)} + h_x^{(2)}) - \lambda_1(h_x^{(1)} + h_x^{(2)}) \geqslant [\lambda_n(h_x^{(2)}) - \lambda_1(h_x^{(2)})] - [\lambda_n(h_x^{(1)}) - \lambda_1(h_x^{(1)})].
$$

Hence, once

$$
[\lambda_n(h_x^{(2)}) - \lambda_1(h_x^{(2)})] \geqslant 2[\lambda_n(h_x^{(1)}) - \lambda_1(h_x^{(1)})],
$$

we have

$$
J(U_x) \geqslant J(U_x^{(1)}).
$$

Remark 3. Proposition 1 provides a design guide for the control Hamiltonian $H_c^{(i)}$ such that by utilizing multiple encoding channels rather than a single unitary channel, the best possible precision limit of quantum parameter estimation can be improved.

3.2 An illustrative example

Consider a single qubit quantum probe. Denote the jk-th ($1 \leqslant j, k \leqslant 2$) element of the matrix of $h_x^{(i)}$ (for $i = 1, 2$) as $h_{jk}^{(i)}$, where the subscript x is omitted. The eigenpolynomial of $h_x^{(1)} + h_x^{(2)}$ is

$$
\det[\lambda I - (h_x^{(1)} + h_x^{(2)})] = \lambda^2 - (h_{11}^{(1)} + h_{22}^{(1)} + h_{11}^{(2)} + h_{22}^{(2)})\lambda
$$
$$
+ (h_{11}^{(1)} + h_{11}^{(2)})(h_{22}^{(1)} + h_{22}^{(2)}) - |h_{12}^{(1)} + h_{12}^{(2)}|^2.
$$

Thus, the quantum Fisher information $J(U_x)$ of the total encoding channel can be calculated as

$$
[\lambda_n(h_x^{(1)} + h_x^{(2)}) - \lambda_1(h_x^{(1)} + h_x^{(2)})]^2
$$
$$
= [\lambda_n(h_x^{(1)}) - \lambda_1(h_x^{(1)})]^2 + [\lambda_n(h_x^{(2)}) - \lambda_1(h_x^{(2)})]^2
$$
$$
+ 2(h_{11}^{(1)} - h_{22}^{(1)})(h_{11}^{(2)} - h_{22}^{(2)}) + 4(h_{12}^{(1)} h_{12}^{(2)\dagger} + h_{12}^{(2)} h_{12}^{(1)\dagger})
$$
$$
= [\lambda_n(h_x^{(1)}) - \lambda_1(h_x^{(1)})]^2 + 2(h_{11}^{(1)} - h_{22}^{(1)})(h_{11}^{(2)} - h_{22}^{(2)})
$$
$$
+ (h_{11}^{(2)} - h_{22}^{(2)})^2 + 4(h_{12}^{(1)} h_{12}^{(2)\dagger} + h_{12}^{(2)} h_{12}^{(1)\dagger} + |h_{12}^{(2)}|^2), \tag{14}
$$

where the equality

$$
[\lambda_n(h_x^{(i)}) - \lambda_1(h_x^{(i)})]^2 = (h_{11}^{(i)} + h_{22}^{(i)})^2 - 4(h_{11}^{(i)} h_{22}^{(i)} - |h_{12}^{(i)}|^2)
$$

is applied.

In the first equality of (14), the first and second terms are the quantum Fisher information of the channels $U_x^{(1)}$ and $U_x^{(2)}$, respectively, when they are utilized to encode the parameter separately. The third term depends on both $U_x^{(1)}$ and $U_x^{(2)}$ depicting their cooperation. Thus in addition to $J(U_x^{(1)})$ and $J(U_x^{(2)})$, the quantum Fisher information of the entire encoding channel $J(U_x)$ also involves an interaction part that describes the cooperation between the separate channels. This is a typical quantum interference effect.

From the second equality in (14), if $h_x^{(2)}$ satisfies

$$
(h_{11}^{(2)} - h_{22}^{(2)})^2 + 2(h_{11}^{(1)} - h_{22}^{(1)})(h_{11}^{(2)} - h_{22}^{(2)}) + 4(h_{12}^{(1)} h_{12}^{(2)\dagger} + h_{12}^{(2)} h_{12}^{(1)\dagger} + |h_{12}^{(2)}|^2) \geqslant 0, \tag{15}
$$

then $J(U_x) \geqslant J(U_x^{(1)})$.

Moreover, if $H_x^{(2)}$ is in the form of

$$
H_x^{(2)} = \alpha x \sigma_3 = \begin{pmatrix} \alpha x & 0 \\ 0 & -\alpha x \end{pmatrix},
$$

where $\alpha > 0$, then

$$
h_x^{(2)} = t_2 \frac{\partial}{\partial x} H_x^{(2)} = t_2 \begin{pmatrix} \alpha & 0 \\ 0 & -\alpha \end{pmatrix}.
$$

By (15), it can be seen that $J(U_x) \geqslant J(U_x^{(1)})$ if $\alpha t_2 \geqslant \max[h_{22}^{(1)} - h_{11}^{(1)}, 0]$, which shows that the precision limit can be improved by exploiting the positive cooperation effect of the two encoding channels.

3.3 The case with many unitary channels

In this subsection, we focus on the case where a series of unitary channels are employed for quantum sensing.

As illustrated in Figure 3, suppose that there are N sequential encoding channels in total, and $H_x^{(i)}$ is the Hamiltonian of the i-th encoding channel whose duration is t_i, $i = 1, \ldots, N$. The corresponding unitary channel is $U_x^{(i)} = \mathrm{e}^{-\frac{i}{\hbar} H_x^{(i)} \cdot t_i}$. Thus, the entire encoding channel is $U_x = U_x^{(N)} U_x^{(N-1)} \cdots U_x^{(2)} U_x^{(1)}$ with a total duration $T = \sum_{j=1}^{N} t_j$. The following theorem gives the quantum Fisher information $J(U_x)$ of the entire channel U_x.
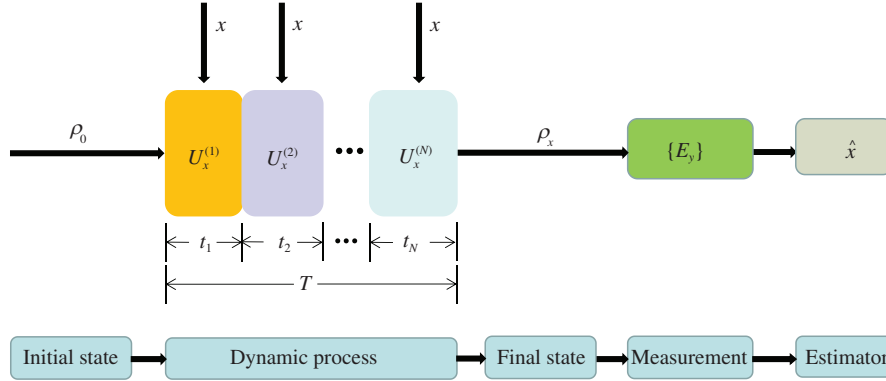
Figure 3 (Color online) Schematic for quantum parameter estimation with sequential unitary encoding channels. The probe prepared in a known initial state ρ_0, is sent through a sequence of channels $U_x^{(i)}$ with the underlying Hamiltonian $H_x^{(i)}$ for a duration of t_i, $i = 1, \ldots, N$. After that, a measurement is implemented on the final state, and then an estimation $\hat{x}$ of the parameter x is given from the measurement results.

Theorem 2. The quantum Fisher information of the entire encoding channel is

$$J(U_x) = [\lambda_{\max}(\bar{h}_x) - \lambda_{\min}(\bar{h}_x)]^2,$$

where $\bar{h}_x = i[\bar{U}_x^\dagger U_x^{(N)\dagger}(\partial_x U_x^{(N)})\bar{U}_x + \bar{U}_x^\dagger \partial_x \bar{U}_x + (\partial_x U_x^{(1)})U_x^{(1)\dagger}]$, and $\bar{U}_x = U_x^{(N-1)} \cdots U_x^{(2)}$. If

$$[\lambda_{\max}(\bar{h}_x) - \lambda_{\min}(\bar{h}_x)] \geqslant [\lambda_{\max}(h_x^{(1)}) - \lambda_{\min}(h_x^{(1)})],$$

then $J(U_x) \geqslant J(U_x^{(1)})$.

Proof. According to (1), we need to calculate $C_\theta(U_x^\dagger U_{x+dx})$. By (2) and the property of eigenvalues of product matrices, it can be verified that

$$
\begin{aligned}
C_\theta(U_x^\dagger U_{x+dx}) &= C_\theta(U_x^{(1)\dagger} U_x^{(2)\dagger} \cdots U_x^{(N-1)\dagger} U_x^{(N)\dagger} U_{x+dx}^{(N)} U_{x+dx}^{(N-1)} \cdots U_{x+dx}^{(2)} U_{x+dx}^{(1)}) \\
&= C_\theta([U_x^{(2)\dagger} \cdots U_x^{(N-1)\dagger}][U_x^{(N)\dagger} U_{x+dx}^{(N)}][U_{x+dx}^{(N-1)} \cdots U_{x+dx}^{(2)}][U_{x+dx}^{(1)} U_x^{(1)\dagger}]). \quad (16)
\end{aligned}
$$

Noting that $\bar{U}_x = U_x^{(N-1)} \cdots U_x^{(2)}$, Eq. (16) can be expressed as

$$C_\theta(U_x^\dagger U_{x+dx}) = C_\theta(\bar{U}_x^\dagger [U_x^{(N)\dagger} U_{x+dx}^{(N)}]\bar{U}_{x+dx}[U_{x+dx}^{(1)} U_x^{(1)\dagger}]).$$

Expand the terms in the parenthesis of the above equation to the first order of dx, and we have

$$
\begin{aligned}
&\bar{U}_x^\dagger [U_x^{(N)\dagger} U_{x+dx}^{(N)}]\bar{U}_{x+dx}[U_{x+dx}^{(1)} U_x^{(1)\dagger}] \\
&= I + [\bar{U}_x^\dagger U_x^{(N)\dagger}(\partial_x U_x^{(N)})\bar{U}_x + \bar{U}_x^\dagger \partial_x \bar{U}_x + (\partial_x U_x^{(1)})U_x^{(1)\dagger}]dx + o(dx) \\
&= I - i\bar{h}_x dx + o(dx) \\
&= e^{-i\bar{h}_x dx} + o(dx),
\end{aligned}
$$

where $\bar{h}_x = i[\bar{U}_x^\dagger U_x^{(N)\dagger}(\partial_x U_x^{(N)})\bar{U}_x + \bar{U}_x^\dagger \partial_x \bar{U}_x + (\partial_x U_x^{(1)})U_x^{(1)\dagger}]$. Thus, by combing (1) and (2), the quantum Fisher information of the entire encoding channel is

$$J(U_x) = [\lambda_{\max}(\bar{h}_x) - \lambda_{\min}(\bar{h}_x)]^2.$$

Thus, it is clear that if $[\lambda_{\max}(\bar{h}_x) - \lambda_{\min}(\bar{h}_x)] \geqslant [\lambda_{\max}(h_x^{(1)}) - \lambda_{\min}(h_x^{(1)})]$, then $J(U_x) \geqslant J(U_x^{(1)})$.

Remark 4. Note that here we only consider the precision limits of the entire channel (N sequential encoding channels in total) and the first unitary encoding channel only for simplicity. It is worth pointing out that for other parameter-encoding processes such as channels consisting of the first n sequential sensing channels, where $n = 2, \ldots, N-1$, the methods presented in Theorems 1 and 2 can also be applied to calculate the corresponding quantum channel Fisher information, and further to compare their precision limits. Particularly, one can also compare the precision limit of the channel $U_x(T) = e^{-\frac{i}{\hbar}H_x \cdot T}$ whose
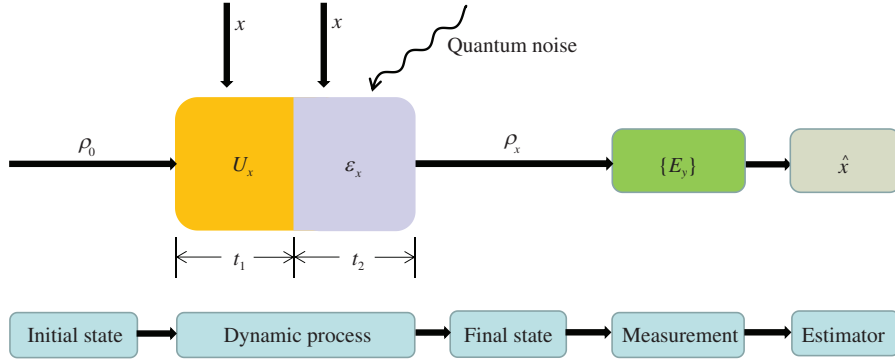
Figure 4 (Color online) Schematic for quantum parameter estimation in the case where the encoding channel is a unitary channel followed by a non-unitary channel. The probe prepared in a known initial state ρ_0, is first sent through a unitary encoding channel U_x for a duration t_1, and then a non-unitary channel ε_x for a period t_2. After that, a measurement is implemented on the final state, and then an estimate $\hat{x}$ of the parameter x is given from the measurement results.

duration is also T. By (10) in Theorem 1, it is not difficult to obtain the quantum Fisher information of $U_x(T)$ being $J(U_x(T)) = [\lambda_{\max}(h_x) - \lambda_{\min}(h_x)]^2$, where

$$h_x = \int_0^T \exp\left(-\frac{i}{\hbar}sH_x\right)\left(\frac{\partial}{\partial x}H_x\right)\exp\left(\frac{i}{\hbar}sH_x\right)\mathrm{d}s.$$

This quantity $J(U_x(T))$ can be further compared with $J(U_x)$.

4 Quantum channel Fisher information of non-unitary channels

In this section, we consider the case where the multiple channels are a unitary channel U_x followed by a non-unitary channel ε_x.

4.1 The case with unitary-non-unitary-channel

Recall that a quantum system must be treated as an open system once the sensing time is comparable with the coherence time. Thus the entire encoding process can be viewed as a unitary evolution followed by a non-unitary evolution.

As shown in Figure 4, the probe prepared in state ρ_0 is first sent through the encoding channel $U_x(t_1) = \mathrm{e}^{-\frac{i}{\hbar}H_x \cdot t_1}$, and then the non-unitary channel $\varepsilon_x(\rho) = \sum_i k_i(x, t_2)\rho k_i^\dagger(x, t_2)$ with a duration t_2, where $\rho = U_x(t_1)\rho_0 U_x^\dagger(t_1)$, and the set of Kraus operators $\{k_i(x, t)\}$ satisfy $\sum_i k_i^\dagger(x, t)k_i(x, t) = I$. Thus at the end of the entire encoding dynamics, the final state of the probe becomes $\rho_x = \sum_i F_i(x, t)\rho_0 F_i^\dagger(x, t)$, where

$$F_i(x, t) = k_i(x, t_2)U_x(t_1)$$

satisfy $\sum_i F_i^\dagger(x, t)F_i(x, t) = I$, and $t = t_1 + t_2$. The quantum Fisher information of the entire multiple channels can be calculated as [47]

$$J(U_x, \varepsilon_x) = \lim_{dx \to 0} \frac{8(1 - \max_{||W|| \leqslant 1}\frac{1}{2}\lambda_{\min}(F_W + F_W^\dagger))}{dx^2}, \tag{17}$$

where $F_W = \sum_{i,j} w_{ij}F_i^\dagger(x, t)F_j(x + dx, t)$, and w_{ij} is the ij-th element of the matrix W.

In practical quantum metrology, the open dynamics ε_x may depend on the unitary evolution U_x through the Kraus operators in the form of [47, 56–58]

$$k_i(x, t_2) = A_i(\eta(t_2))U_x(t_2), \tag{18}$$

where $A_i(\eta(t))$ and $\eta(t)$ depict the corresponding quantum noise and satisfy $\sum_i A_i^\dagger(\eta(t))A_i(\eta(t)) = I$. In Subsection 4.2, we will consider five typical noisy quantum channels and three different forms of $\eta(t)$. With quantum noise as (18), the final state of the probe becomes $\rho_x = \sum_i F_i(x, t)\rho_0 F_i^\dagger(x, t)$ where

$$F_i(x, t) = A_i(\eta(t_2))U_x(t),$$

Table 1 The quantum Fisher information of typical noisy quantum channels. The first three columns describe the five typical noisy quantum channels, in which the noise parameter $\eta(t)$ satisfies $0 \leqslant \eta(t) \leqslant 1$. The fourth column gives the quantum Fisher information of the unitary encoding channel $U_x(t) = \mathrm{e}^{-\frac{i}{\hbar}H_x \cdot t}$. The last column is the quantum Fisher information of the entire encoding channel

	$A_1(\eta(t))$	$A_2(\eta(t))$	$J(U_x)$ $t \in [0, t_1]$	$J(U_x, \varepsilon_x)$ $t \in [t_1, t_2]$
Bit flip	$\sqrt{1-\eta(t)}\begin{pmatrix} 1 & 0 \\ 0 & 1 \end{pmatrix}$	$\sqrt{\eta(t)}\begin{pmatrix} 0 & 1 \\ 1 & 0 \end{pmatrix}$	t^2	$[1-2\eta(t-t_1)]^2 t^2$
Phase flip	$\sqrt{1-\eta(t)}\begin{pmatrix} 1 & 0 \\ 0 & 1 \end{pmatrix}$	$\sqrt{\eta(t)}\begin{pmatrix} 1 & 0 \\ 0 & -1 \end{pmatrix}$	t^2	$[1-2\eta(t-t_1)]^2 t^2$
Amplitude damping	$\begin{pmatrix} 1 & 0 \\ 0 & \sqrt{1-\eta(t)} \end{pmatrix}$	$\begin{pmatrix} 0 & \sqrt{\eta(t)} \\ 0 & 0 \end{pmatrix}$	t^2	$\frac{4[1-\eta(t-t_1)]t^2}{[1+\sqrt{1-\eta(t-t_1)}]^2}$
Phase damping	$\begin{pmatrix} 1 & 0 \\ 0 & \sqrt{1-\eta(t)} \end{pmatrix}$	$\begin{pmatrix} 0 & 0 \\ 0 & \sqrt{\eta(t)} \end{pmatrix}$	t^2	$[1-\eta(t-t_1)]t^2$
Bit-phase flip	$\sqrt{1-\eta(t)}\begin{pmatrix} 1 & 0 \\ 0 & 1 \end{pmatrix}$	$\sqrt{\eta(t)}\begin{pmatrix} 0 & -i \\ i & 0 \end{pmatrix}$	t^2	$[1-2\eta(t-t_1)]^2 t^2$

and $t = t_1 + t_2$. Thus Eq. (17) can be applied to obtain the quantum Fisher information $J(U_x, \varepsilon_x)$ of the entire multiple channels, and this can be further compared with $J(U_x)$, which is the quantum channel Fisher information of the unitary encoding part only.

4.2 Typical noisy quantum channels

To demonstrate the characteristics of the quantum channel Fisher information of unitary-non-unitary channels, we first specify the unitary channel as $U_x(t) = \mathrm{e}^{-\frac{i}{\hbar}H_x \cdot t}$, where $H_x = \frac{\sigma_3}{2}x$, and σ_3 is the Pauli matrix. Then for the non-unitary channel ε_x, suppose that $\varepsilon_x(\rho) = \sum_i k_i(x, t_2)\rho k_i^\dagger(x, t_2)$, where $k_i(x, t_2) = A_i(\eta(t_2))U_x(t_2)$ as in (18).

As detailed in Table 1, we consider five typical noisy quantum channels: bit flip channel, phase flip channel, amplitude damping channel, phase damping channel, and bit-phase flip channel, described by the corresponding Kraus operators $\{A_i\}$. Note that as $\eta(t)$ approaches 0 continuously, the non-unitary channel ε_x approaches the unitary channel U_x in a continuous way.

If the sensing time $t \leqslant t_1$, the encoding dynamics is unitary, and the corresponding quantum channel Fisher information can be calculated as $J(U_x) = t^2$. While if $t > t_1$, the quantum Fisher information of the unitary-non-unitary channel can be derived by (17). For different noisy quantum channels, the quantum Fisher information $J(U_x, \varepsilon_x)$ of the entire encoding channel is detailed in the last column of Table 1. It can be seen that $J(U_x, \varepsilon_x)$ depends on the noise parameter $\eta(t)$. Generally, $\eta(t)$ has the following three typical forms: (i) $\eta(t) = \eta$; (ii) $\eta(t) = 1 - \mathrm{e}^{-2\gamma t}$, where γ depicts the spontaneous emission rate; (iii) $\eta(t) = 1 - \cos^2(\alpha t)$, where α represents the coupling strength between the system and its environment.

To illustrate the impact of the parameter $\eta(t)$, we plot the quantum channel Fisher information with different noise parameters $\eta(t)$ in Figure 5. In Figures 5(a)–(c), the noisy channel is the phase damping channel, while in Figure 5(d), the noisy channel is the phase flip channel. The noise parameters $\eta(t)$ are $\eta(t) = \eta$, $\eta(t) = 1 - \mathrm{e}^{-2\gamma t}$, and $\eta(t) = 1 - \cos^2(\alpha t)$ with corresponding different parameters in Figures 5(a)–(c), respectively. Here, the switch time t_1 is set to be 2.

As can be seen from Figures 5(a) and (d), if the noise parameter $\eta(t)$ is constant, there is a sudden decrease of the quantum channel Fisher information at the switch time $t_1 = 2$, from which an open system dynamics replaces the preceding unitary evolution. In Figure 5(a), for the quantum phase damping noise, $J(U_x, \varepsilon_x) = (1 - \eta)t^2$. Thus the bigger the noise parameter η is, the more the quantum channel Fisher information decreases at the time t_1. Since the sensing time is a valuable resource, as the sensing time increases, the quantum Fisher information $J(U_x, \varepsilon_x)$ of the entire encoding channel gradually exceeds the value of $J(U_x)$ at the switch time t_1. For the phase flip noise in Figure 5(d), $J(U_x, \varepsilon_x) = (1 - 2\eta)^2 t^2$. Hence, for $\eta = 0.5$, the quantum channel Fisher information $J(U_x, \varepsilon_x)$ drops to 0 suddenly at the switch time t_1, and remains to be 0. In this case, there is no information at all of x being contained in the final state of the entire encoding channel, no matter how long is the encoding period. For other values of the noise parameter η, as extending the sensing time, $J(U_x, \varepsilon_x)$ can slowly exceed $J(U_x)$ valued at the switch time t_1. In Figure 5(b), for the noise parameter $\eta(t) = 1 - \mathrm{e}^{-2\gamma t}$, the quantum channel Fisher information $J(U_x, \varepsilon_x)$ will continuously increase after the switch time t_1 to reach its maximum value, and then quickly decreases to 0 in an exponential way. Moreover, the larger the parameter γ is, the smaller
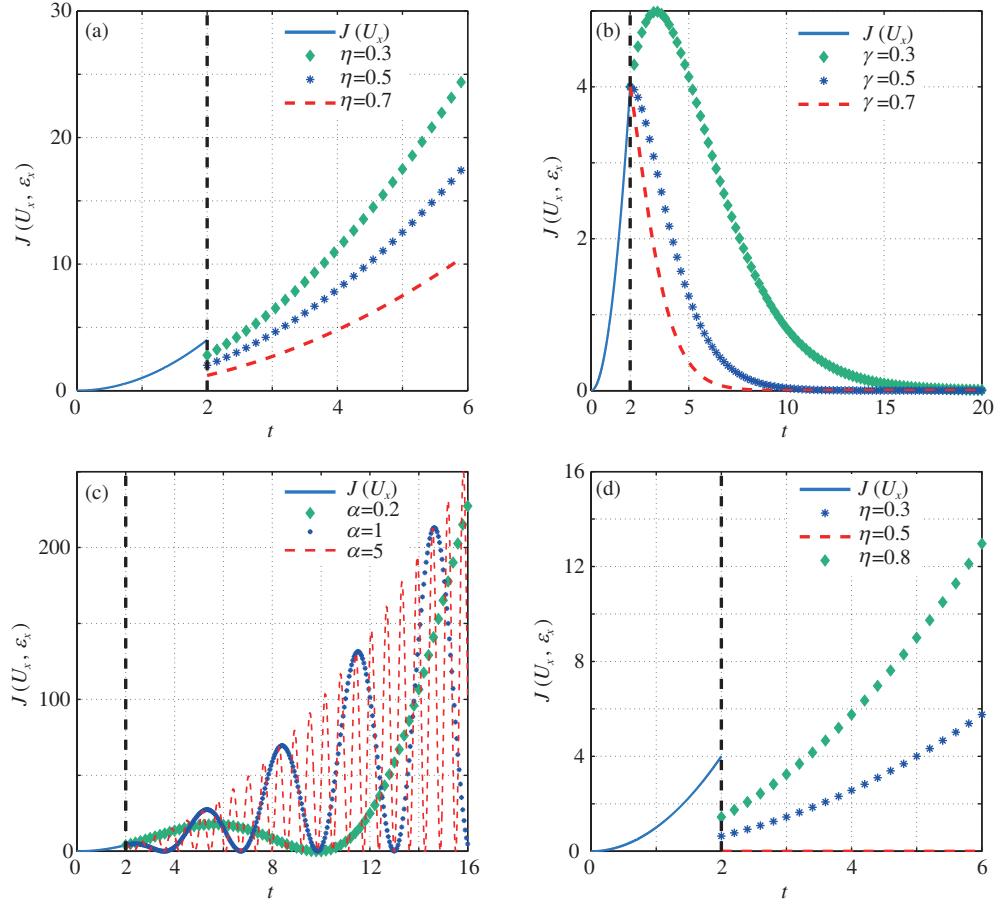
Figure 5 (Color online) The quantum channel Fisher information of $J(U_x)$ and $J(U_x, \varepsilon_x)$ with different noise parameters $\eta(t)$. Here, the switch time $t_1 = 2$. If the encoding time $t \leqslant 2$, the encoding channel is unitary, while for $t > 2$, a noisy encoding channel has to be taken into account. In (a)–(c), the quantum noise is the quantum phase damping noise. The noise parameters $\eta(t)$ are (a) $\eta(t) = \eta$, (b) $\eta(t) = 1 - e^{-2\gamma t}$, and (c) $\eta(t) = 1 - \cos^2(\alpha t)$, respectively. (d) depicts the quantum Fisher information with ε_x being the quantum phase flip noisy channel, and $\eta(t) = \eta$ with different values.

the maximum value of $J(U_x, \varepsilon_x)$ is, and the quicker it decreases. Thus in this case, for large γ, a smart choice of the total encoding time is around the switch time t_1. In Figure 5(c), $\eta(t) = 1 - \cos^2(\alpha t)$, after the switch time t_1, the quantum channel Fisher information $J(U_x, \varepsilon_x)$ starts to oscillate. The larger the parameter α is, the faster $J(U_x, \varepsilon_x)$ oscillates. Although the amplitude of the oscillation increases as the sensing time grows, to extract more information from the entire encoding channel, the sensing time should be determined more precisely.

From this subsection, it can be seen that in practical quantum metrology, the following two points are particularly important: (i) The switch time at which an open system dynamics emerges should be identified; (ii) The total encoding time should be determined precisely to ensure that more information can be extracted from the entire encoding channel.

5   Conclusion

In this paper, we studied the quantum Fisher information of parameter estimation using multiple channels. For several typical kinds of quantum multiple channels, the corresponding quantum channel Fisher information is derived. The results are useful for two important and practical quantum metrology problems: (i) control involved quantum metrology, and (ii) practical quantum metrology where decoherence is unavoidable. For control enhanced quantum metrology, the results can help design controls to improve the quantum channel Fisher information, i.e., to improve the best possible precision limit of quantum parameter estimation. For practical quantum metrology, the results provide a reference for properly choosing the sensing time in presence of a non-unitary channel, under which circumstance the quantum

channel Fisher information may decrease for a long sensing time. We expect that our results may trigger more studies on the quantum parameter estimation with multiple channels.

References

1 Giovannetti V, Lloyd S, Maccone L. Quantum metrology. Phys Rev Lett, 2006, 96: 010401
2 Xiang G Y, Higgins B L, Berry D W, et al. Entanglement-enhanced measurement of a completely unknown optical phase. Nat Photon, 2011, 5: 43–47
3 Napolitano M, Koschorreck M, Dubost B, et al. Interaction-based quantum metrology showing scaling beyond the Heisenberg limit. Nature, 2011, 471: 486–489
4 Escher B M, de Matos Filho R L, Davidovich L. Quantum metrology for noisy systems. Braz J Phys, 2011, 41: 229–247
5 Demkowicz-Dobrzański R, Kołodyński J, Guţă M. The elusive Heisenberg limit in quantum-enhanced metrology. Nat Commun, 2012, 3: 1063
6 Kołodyński J, Demkowicz-Dobrzański R. Efficient tools for quantum metrology with uncorrelated noise. New J Phys, 2013, 15: 073043
7 Escher B M, de Matos Filho R L, Davidovich L. General framework for estimating the ultimate precision limit in noisy quantum-enhanced metrology. Nat Phys, 2011, 7: 406–411
8 Alipour S, Mehboudi M, Rezakhani A T. Quantum metrology in open systems: dissipative Cramér-Rao bound. Phys Rev Lett, 2014, 112: 120405
9 Liu Z P, Zhang J, Özdemir K, et al. Metrology with PT-symmetric cavities: enhanced sensitivity near the PT-phase transition. Phys Rev Lett, 2016, 117: 110802
10 Hou Z B, Zhu H J, Xiang G Y, et al. Achieving quantum precision limit in adaptive qubit state tomography. npj Quantum Inf, 2016, 2: 16001
11 Zhang J, Peng B, Özdemir K, et al. A phonon laser operating at an exceptional point. Nat Photon, 2018, 12: 479–484
12 Wang Y L, Dong D Y, Qi B, et al. A quantum hamiltonian identification algorithm: computational complexity and error analysis. IEEE Trans Autom Control, 2018, 63: 1388–1403
13 Yokoyama S, Pozza N D, Serikawa T, et al. Characterization of entangling properties of quantum measurement via two-mode quantum detector tomography using coherent state probes. Opt Express, 2019, 27: 34416–34432
14 Wang Y L, Yin Q, Dong D Y, et al. Quantum gate identification: error analysis, numerical results and optical experiment. Automatica, 2019, 101: 269–279
15 Hou Z, Wang R J, Tang J F, et al. Control-enhanced sequential scheme for general quantum parameter estimation at the Heisenberg limit. Phys Rev Lett, 2019, 123: 040501
16 Song Q J, Huang Z Y. Identification of errors-in-variables systems with general nonlinear output observations and with ARMA observation noises. J Syst Sci Complex, 2020, 33: 1–14
17 Hou Z B, Zhang Z, Xiang G Y, et al. Minimal tradeoff and ultimate precision limit of multiparameter quantum magnetometry under the parallel scheme. Phys Rev Lett, 2020, 125: 020501
18 Hou Z B, Tang J F, Ferrie C, et al. Experimental realization of self-guided quantum process tomography. Phys Rev A, 2020, 101: 022317
19 Wang Y L, Dong D Y, Sone A, et al. Quantum Hamiltonian identifiability via a similarity transformation approach and beyond. IEEE Trans Autom Control, 2020, 65: 4632–4647
20 Yu Q, Wang Y L, Dong D Y, et al. On the capability of a class of quantum sensor. 2020. ArXiv:2003.08679
21 Liu L Q, Yuan H D. Achieving higher precision in quantum parameter estimation with feedback controls. Phys Rev A, 2020, 102: 012208
22 Roy S M, Braunstein S L. Exponentially enhanced quantum metrology. Phys Rev Lett, 2008, 100: 220501
23 Anisimov P M, Raterman G M, Chiruvelli A, et al. Quantum metrology with two-mode squeezed vacuum: parity detection beats the Heisenberg limit. Phys Rev Lett, 2010, 104: 103602
24 Chaves R, Brask J B, Markiewicz M, et al. Noisy metrology beyond the standard quantum limit. Phys Rev Lett, 2013, 111: 120401
25 Demkowicz-Dobrzański R, Maccone L. Using entanglement against noise in quantum metrology. Phys Rev Lett, 2014, 113: 250801
26 Yuan H. Sequential feedback scheme outperforms the parallel scheme for Hamiltonian parameter estimation. Phys Rev Lett, 2016, 117: 160801
27 Giovannetti V. Quantum-enhanced measurements: beating the standard quantum limit. Science, 2004, 306: 1330–1336
28 Choi S, Sundaram B. Bose-einstein condensate as a nonlinear Ramsey interferometer operating beyond the Heisenberg limit. Phys Rev A, 2008, 77: 053613
29 Giovannetti V, Lloyd S, Maccone L. Advances in quantum metrology. Nat Photon, 2011, 5: 222–229
30 Yuan H D, Fung C H F. Optimal feedback scheme and universal time scaling for Hamiltonian parameter estimation. Phys Rev Lett, 2015, 115: 110401
31 Liu J, Yuan H D. Quantum parameter estimation with optimal control. Phys Rev A, 2017, 96: 012117
32 Pang S, Jordan A N. Optimal adaptive control for quantum metrology with time-dependent Hamiltonians. Nat Commun, 2017, 8: 14695
33 Matsuzaki Y, Benjamin S, Nakayama S, et al. Quantum metrology beyond the classical limit under the effect of dephasing. Phys Rev Lett, 2018, 120: 140501
34 Wang K K, Wang X P, Zhan X, et al. Entanglement-enhanced quantum metrology in a noisy environment. Phys Rev A, 2018, 97: 042112
35 Chen Y, Yuan H D. Cooperation between coherent controls and noises in quantum metrology. 2018. ArXiv:1801.07563v1
36 Zhou S S, Zhang M Z, Preskill J, et al. Achieving the Heisenberg limit in quantum metrology using quantum error correction. Nat Commun, 2018, 9: 78
37 Liu L J, Cheng S M, Qi B, et al. Precision limit of atomic magnetometers in the presence of spin-destruction collisions. J Phys B-At Mol Opt Phys, 2015, 48: 035502

38 Liu L J, Qi B, Cheng S M, et al. High precision estimation of inertial rotation via the extended Kalman filter. Eur Phys J D, 2015, 69: 261

39 Wu C Z, Qi B, Chen C L, et al. Robust learning control design for quantum unitary transformations. IEEE Trans Cybern, 2017, 47: 4405–4417

40 Gong B L, Cui W. Multi-objective optimization in quantum parameter estimation. Sci China-Phys Mech Astron, 2018, 61: 040312

41 Gong B L, Yang Y, Cui W. Quantum parameter estimation via dispersive measurement in circuit QED. Quantum Inf Process, 2018, 17: 301

42 Dong D Y, Xing X, Ma H L, et al. Learning-based quantum robust control: algorithm, applications, and experiments. IEEE Trans Cybern, 2020, 50: 3581–3593

43 Liu J, Yuan H D, Lu X M, et al. Quantum Fisher information matrix and multiparameter estimation. 2019. ArXiv:1907.08037

44 Holevo A. Probabilistic and Statistical Aspects of Quantum Theory. Amsterdam: Edizioni della Normale, 1982

45 Braunstein S L, Caves C M, Milburn G J. Generalized uncertainty relations: theory, examples, and Lorentz invariance. Ann Phys, 1996, 247: 135–173

46 Braunstein S L, Caves C M. Statistical distance and the geometry of quantum states. Phys Rev Lett, 1994, 72: 3439–3443

47 Yuan H D, Fung C H F. Quantum parameter estimation with general dynamics. npj Quantum Inf, 2017, 3: 14

48 Pang S S, Brun T A. Quantum metrology for a general Hamiltonian parameter. Phys Rev A, 2014, 90: 022117

49 Anis A, Lvovsky A I. Maximum-likelihood coherent-state quantum process tomography. New J Phys, 2012, 14: 105021

50 Qi B, Hou Z B, Li L, et al. Quantum state tomography via linear regression estimation. Sci Rep, 2013, 3: 3496

51 Qi B, Hou Z B, Wang Y L, et al. Adaptive quantum state tomography via linear regression estimation: Theory and two-qubit experiment. npj Quantum Inf, 2017, 3: 19

52 Yuan H D, Fung C H F. Fidelity and Fisher information on quantum channels. New J Phys, 2017, 19: 113039

53 Wilcox R M. Exponential operators and parameter differentiation in quantum physics. J Math Phys, 1967, 8: 962–982

54 Scully M O, Zubairy M S. Quantum Optics. Cambridge: Cambridge University Press, 1997

55 Zhang X D. Matrix Analysis and Applications. Cambridge: Cambridge University Press, 2017

56 Liu Y, Cui J X. Realization of Kraus operators and POVM measurements using a duality quantum computer. Chin Sci Bull, 2014, 59: 2298–2301

57 Meng X G, Wang J S, Gao H C. Kraus operator-sum solution to the master equation describing the single-mode cavity driven by an oscillating external field in the heat reservoir. Int J Theor Phys, 2016, 55: 3630–3636

58 Ruan L Z, Dai W H, Win M Z. Adaptive recurrence quantum entanglement distillation for two-Kraus-operator channels. Phys Rev A, 2018, 97: 052332